Available online at www.sciencedirect.com
SCIENCE DIRECT®
Journal of Sound and Vibration 278 (2004) 501–526
JOURNAL OF SOUND AND VIBRATION
www.elsevier.com/locate/jsvi

Plane wave propagation and frequency band gaps in periodic plates and cylindrical shells with and without heavy fluid loading

S.V. Sorokin[a,*], O.A. Ershova[b]

[a] *Center of Machine Acoustic, Institute of Mechanical Engineering, Aalborg University, Pontoppidanstraede 101, DK 9220 Aalborg, Denmark*

[b] *Department of Engineering Mechanics, State Marine Technical University of St. Petersburg, St. Petersburg 190008, Russia*

Received 19 May 2003; accepted 8 October 2003

Abstract

Free plane wave propagation in infinitely long periodic elastic structures with and without heavy fluid loading is considered. The structures comprise continuous elements of two different types connected in an alternating sequence. In the absence of fluid loading, an exact solution which describes wave motion in each unboundedly extended element is obtained analytically as a superposition of all propagating and evanescent waves, continuity conditions at the interfaces between elements are formulated and standard Floquet theory is applied to set up a characteristic determinant. An efficient algorithm to compute Bloch parameters (propagation constants) as a function of the excitation frequency is suggested and the location of band gaps is studied as a function of non-dimensional parameters of the structure's composition. In the case of heavy fluid loading, an infinitely large number of propagating or evanescent waves exist in each unboundedly extended elasto-acoustic element of a periodic structure. Wave motion in each element is then presented in the form of a modal decomposition with a finite number of terms retained in these expansions and the accuracy of such an approximation is assessed. A generalized algorithm is used to compute Bloch parameters for a periodic structure with heavy fluid loading as a function of the excitation frequency and, similarly to the previous case, the location of band gaps is studied.

*Corresponding author.
E-mail address: svs@ime.auc.dk (S.V. Sorokin).

0022-460X/$ - see front matter © 2003 Elsevier Ltd. All rights reserved.
doi:10.1016/j.jsv.2003.10.042

1. Introduction

The propagation of waves in a periodic wave guide is a classic problem in structural dynamics which has been extensively studied by many authors (see, for example, Refs. [1,2]). As is well known, it is typical for periodic structures to have several 'stop bands' or 'band gaps' in the frequency domain, where no wave propagation is possible. This physical phenomenon is very important for many practical applications, in which a sufficiently long periodic structure (e.g., a pipeline with multiple supports) is exposed to driving forces applied within a relatively compact excitation zone. In certain situations such a structure exhibits resonant motions which are strongly localized in this zone and no energy is transmitted to other parts of the structure. A comprehensive review of work on wave propagation and band gaps in periodic structures is available, for example, in Ref. [3]. The 'trapping' and 'stop band' phenomena in structural dynamics has been analyzed, for example in Refs. [4–7], for an infinitely long rod or a beam with periodically spaced point supports or concentrated masses, for an infinitely long cylindrical shell and for a regularly perturbed acoustical wave guide. Refs. [4–6], similarly to many others discussed in Ref. [3], deal with a 'lumped parameter modelling' of the elements inserted between elastic components of a periodic structure. Wave propagation in a two-dimensional elastic medium filled by the regular arrays of circular inclusions has been analyzed in Refs. [8,9]. The survey of research papers dealing with discrete periodic structures may be found in Ref. [10]. A general overview of the problems of this type is presented, for example, in Ref. [11].

As is seen from this brief review, in the literature the band gap phenomenon in periodic mechanical systems has been explored with respect either to the propagation of elastic waves (solid dynamics) or to the propagation of acoustic waves (fluid dynamics) in periodic wave guides. In practice, a periodic structure composed of continuous elastic segments may be loaded by a 'uniform' acoustic medium and it is necessary to control wave propagation in such a strongly coupled structural-acoustic wave guide (an elastic structure with heavy fluid loading [12]); see, for example, Ref. [3]. This problem arises, as already mentioned, with respect to dynamics of pipelines, assembled by self-repeating alternating elements and exposed to heavy internal fluid loading. To the best of the author's knowledge, the propagation of waves in continuous periodic structures with heavy fluid loading has not yet received attention in the literature, since this problem is mathematically rather involved to obtain a simple analytical solution, whereas the analysis by standard numerical methods (such as FEM) requires extensive and time-consuming computations. It should also be pointed out that the vast majority of research papers in the subject concern a stiffened elastic structure (i.e., a plate or a cylindrical shell) whereas the present paper deals with an alternating sequence of continuous elastic or elasto-acoustic coupled segments, each of which supports the wave propagation.

Specifically, an infinitely long plate and an infinitely long cylindrical shell comprising sets of alternating continuous elements both without and with heavy fluid loading are considered. In the latter case, an acoustic medium is extended unboundedly along the structure. It is either of a finite depth and located at one side of the structure (a plate) or it fills the structure (a cylindrical shell). Wave motion in each elastic or coupled elasto-acoustic element of a periodic structure is sought in the form of a modal decomposition of displacements and (for a fluid-loaded structure) velocity potentials. Continuity conditions at the interfaces between elements are formulated and Floquet theory [13,14] is applied to set up a characteristic equation, which defines the location and the

width of band gaps. The problem being considered concerns a series of relatively long stiff plates or cylinders, alternating with soft gaskets. The analysis is restricted to plane wave propagation and (in the case of a cylindrical shell) to axisymmetric modes. However, the algorithms used for solving the problems are readily extended to capture the similar wave propagation phenomena for point excitation of a plate with periodic co-centred ring inclusions and for a cylindrical shell vibrating at an arbitrary circumferential wave number.

The paper is organized as follows. In Section 2, analysis of the wave propagation in an infinitely long plate composed of an alternating sequence of elements without fluid loading is performed. Exact equations to determine Bloch parameter for given excitation frequency are derived. Two alternative algorithms are used to plot several branches of characteristic curves. The location and the width of band gaps are studied as a function of the parameters of a periodic structure. Similar analysis of the wave propagation in an infinitely long cylindrical shell without fluid loading is performed in Section 3. A shell is composed of the set of elements of two types and analysis of wave motions is restricted by the axisymmetric ('breathing') modes. Section 4 extends the analysis of the wave propagation performed in Section 2 to a plate, which is loaded by an acoustic layer of the constant depth. The location and the width of band gaps for a plate with and without fluid loading are compared in this section. The wave propagation in a cylindrical shell filled by an acoustic medium is analyzed in Section 5 and the contribution of heavy fluid loading to the 'band gap effect' is estimated. The results of analysis are summarized in Section 6.

2. Propagation of flexural waves in a periodic plate composed by a set of alternating elements

An infinitely long plate is composed of the set of periodically repeated (alternating) 'strip' elements of two types shown in Fig. 1. Each set of elements ($j = 1, 2$) is specified by the following parameters: the thickness h_j, the length l_j, Young's modulus E_j, the density ρ_j and Poisson coefficient v_j. Propagation of the stationary plane flexural wave at a circular frequency ω is considered, so that the dynamics of a plate are, in effect, reduced to the dynamics of a beam. It is convenient to introduce the non-dimensional parameters $\Omega = \sqrt{(1-v^2)\rho_1 h_1^2 \omega^2/E_1}$, $\lambda = l_1/h_1$, $\delta = l_2/l_1$, $\alpha = h_2/h_1$, $\beta = \rho_2/\rho_1$, $\chi = E_2/E_1$ (hereafter $v_1 = v_2 \equiv v = 0.3$). The wave motion in the plates is then governed by equations formulated for the lateral displacements w_1, w_2 in the z direction $\left(w_1 = w_1^{\dim}/h_1,\ w_2 = w_2^{\dim}/h_1,\ x = x^{\dim}/h_1\right)$ (see Fig. 1),

$$w_1^{(4)} - 12\Omega^2 w_1 = 0, \quad -\lambda + n\lambda(1+\delta) < x < n\lambda(1+\delta), \quad n = 0, 1, 2, \ldots, \tag{1a}$$

$$w_2^{(4)} - 12\Omega^2 \alpha^{-2}\beta\chi^{-1} w_2 = 0, \quad n\lambda(1+\delta) < x < \lambda\delta + n\lambda(1+\delta), \quad n = 0, 1, 2, \ldots\ . \tag{1b}$$

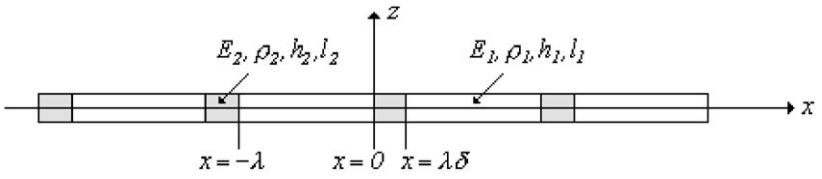

Fig. 1. A periodic plate comprising continuous segments of two types.

General solutions of these equations are sought as ($k_{nj} = k_{nj}^{\dim} h$)

$$w_j(x) = \sum_{n=1}^{4} A_{nj} \exp(\mathrm{i} k_{nj} x), \quad j = 1, 2. \tag{2}$$

The wave numbers in Eq. (2) are explicitly expressed via the frequency parameter as

$$k_{11} = \sqrt[4]{12\Omega^2}, \quad k_{21} = -\sqrt[4]{12\Omega^2}, \quad k_{31} = \mathrm{i}\sqrt[4]{12\Omega^2}, \quad k_{41} = -\mathrm{i}\sqrt[4]{12\Omega^2},$$

$$k_{12} = \sqrt[4]{12\Omega^2\alpha^{-2}\beta\chi^{-1}}, \quad k_{22} = -\sqrt[4]{12\Omega^2\alpha^{-2}\beta\chi^{-1}},$$

$$k_{32} = \mathrm{i}\sqrt[4]{12\Omega^2\alpha^{-2}\beta\chi^{-1}}, \quad k_{42} = -\mathrm{i}\sqrt[4]{12\Omega^2\alpha^{-2}\beta\chi^{-1}}. \tag{3}$$

Matching conditions at the interfaces $x = 0$ and $x = \lambda\delta$ (see Fig. 1) are formulated as the continuity of displacements w, slopes w', bending moments $M \equiv (Eh^2/(12(1-\nu^2)))w''$ and transverse forces $Q \equiv (Eh^2/(12(1-\nu^2)))w'''$ in the non-dimensional form

$$w_1(0) = w_2(0), \quad w_1'(0) = w_2'(0),$$
$$w_1''(0) = \chi\alpha^3 w_2''(0), \quad w_1'''(0) = \chi\alpha^3 w_2'''(0), \tag{4a}$$

$$w_1(\lambda\delta) = w_2(\lambda\delta), \quad w_1'(\lambda\delta) = w_2'(\lambda\delta),$$
$$w_1''(\lambda\delta) = \chi\alpha^3 w_2''(\lambda\delta), \quad w_1'''(\lambda\delta) = \chi\alpha^3 w_2'''(\lambda\delta). \tag{4b}$$

The same conditions are also applied at all other junction points $x = n\lambda(1+\delta)$, $n = 0, 1, 2, \ldots$. Floquet theory [13,14] is used to formulate the periodicity conditions (see Fig. 1)

$$w_1(\lambda\delta) = \exp(\mathrm{i}\mathrm{K}_B) w_1(-\lambda),$$
$$w_1'(\lambda\delta) = \exp(\mathrm{i}\mathrm{K}_B) w_1'(-\lambda),$$
$$w_1''(\lambda\delta) = \exp(\mathrm{i}\mathrm{K}_B) w_1''(-\lambda),$$
$$w_1'''(\lambda\delta) = \exp(\mathrm{i}\mathrm{K}_B) w_1'''(-\lambda). \tag{5}$$

These conditions are substituted in Eqs. (4b) and a system of eight homogeneous equations with respect to eight modal amplitudes grouped in two sets, A_{nj}, $n = 1, 2, 3, 4$, $j = 1, 2$ is derived. This system is rather cumbersome and therefore not presented here. It has a non-trivial solution when its determinant vanishes. This condition formulates a transcendent equation with respect to Bloch parameter K_B, which is a standard variable in the subject, measuring a phase shift in a periodic wave guide [2,11]. It follows from Floquet theory that if all roots of the characteristic equation are complex valued then at a given frequency no propagating waves exist in a periodic plate. In this simple case, it does not present any difficulties to set up the dispersion relation explicitly as a transcendent function of the frequency parameter Ω and the Bloch parameter K_B. The characteristic equation is obtained by equating to zero this dispersion relation,

$$D(\Omega, \mathrm{K}_B) = 0. \tag{6}$$

Then it is possible to formulate either a direct problem of solving the characteristic Eq. (6) (to find the Bloch parameter for a given Ω) or an inverse problem (to find the frequency parameters for a given K_B). From the Floquet theory, wave propagation in a periodic structure is possible only

when the characteristic equation has at least one purely real root K_B for a given Ω. Thus, only these roots should be determined and it is sufficient to consider the interval $0<K_B<\pi$ due to the periodicity of the function $\exp(iK_B)$.

In the 'direct' algorithm, the frequency Ω is used as an input parameter and Eq. (6), which is therefore reduced to $D(K_B)=0$, is solved to find real-valued roots $0<K_B<\pi$ for a given Ω. Then it is necessary to 'sweep' all the frequency range to plot branches of characteristic curve $K_B(\Omega)$ 'one by one'. Use of the inverse formulation makes it possible to plot all branches $\Omega(K_B)$ simultaneously. The characteristic Eq. (6) involves exponents of purely real or purely imaginary argument, which contain the frequency parameter Ω, see formulae for wave numbers (3). At relatively low frequencies, $\Omega<1$ (i.e., when Kirchhoff plate theory is applicable), these exponents of small or moderate argument may conveniently be expanded into power series in Ω. Then Eq. (6), which is reduced to $D(\Omega)=0$ for any given K_B, becomes polynomial one in the frequency parameter. It facilitates an efficient solution of the inverse problem, because a polynomial equation is easily solved by use of standard software, e.g., Mathematica [15], and all positive roots are easily selected. Although this inverse formulation is approximate, its the accuracy is readily assessed by comparison with results obtained with more time-consuming solutions of the direct problem.

In Fig. 2, a typical set of characteristic curves $p(K_B)$ is presented. The non-dimensional frequency parameter is $p=\Omega\sqrt{12}\lambda^2\equiv\sqrt{12(1-\nu^2)\rho_1\omega^2 l_1^4/(E_1h_1^2)}$. In this example (as in all other ones reported in the paper) the Kirchhoff theory is equally applicable to describe wave propagation in both the 'long' and the 'short' elements. As shown by the horizontal straight lines in Fig. 2a, there are two band gaps located between the first and the second and between the second and the third branches, $3.09<p<9.09$, $22.4<p<35.8$. These curves are plotted by a use of the inverse formulation with 24 terms retained in power series expansions of the exponents and they do not differ at all from the curves obtained in the direct formulation in frequency parameter 'sweeping', which involves computations of transcendent functions of wave numbers. All roots K_B of Eq. (6) are complex valued in a band gap and all waves are attenuated. Obviously, the decay rate of a wave defined by a quantity $\mathrm{Min}|\mathrm{Im}\,K_B|$ is frequency-dependent. In Fig. 2b, this dependence is shown. As expected, the decay rate is fairly low in the vicinity of the boundaries of stop bands. However, it grows very rapidly toward the middle of a band gap and reaches a rather large magnitude there. Indeed, at $\mathrm{Min}|\mathrm{Im}\,K_B|=0.5$ the amplitude of a wave decays approximately in 40% whilst passing a single periodicity element from $x=-\lambda$ to $\lambda\delta$ (see Fig. 1).

There are several parameters, which control the difference between plate elements. Here only the role of the stiffness ratio parameter χ is explored in the case, when stiff plate elements have a fixed length, whereas a length of each soft element (a 'gasket') may vary. In Fig. 3, curves 1, 3 and 2, 4 display lower and upper boundaries of the band gaps as functions of $\log_{10}(\chi)$, respectively. Apparently, the band gaps become more narrower as the stiffness ratio tends to unity, $\chi\to1$ (e.g., when the plate elements become identical), so that all branches merge at $\chi=1$. However, the band gaps are not monotonously broadened as this parameter diminishes. The width of each band gap reaches its maximum at χ of some specific magnitude, which is not the same for the first and the second band gap. Then band gaps become narrower and a 'critical' stiffness ratio χ_{cr} may be found for each value of δ, when the curves 3 and 4 almost merge and the second band gap disappears. As is seen from these graphs, if the stiffness parameter continues to diminish, $\chi<\chi_{cr}$,

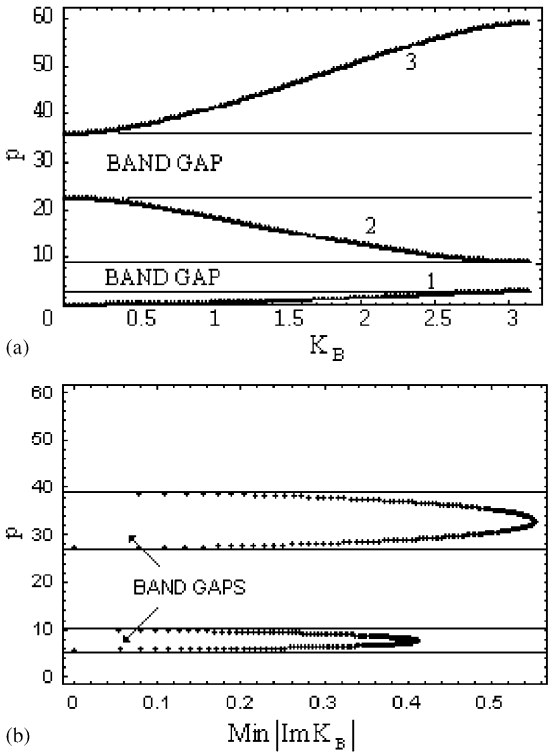

Fig. 2. Characteristic curves and band gaps in a periodic plate ($\alpha = 1$, $\beta = 1$, $\lambda = 200$, $\delta = 0.04$, $\chi = 0.01$) without fluid loading: (a) purely real branches; (b) purely imaginary branches.

the second band gap broadens again. The magnitude of χ_{cr} grows with a growth in the length parameter δ. To conclude a brief discussion of this simple case, it should be pointed out that both the location and the width of band gaps are very sensitive to variations of the parameters of plate elements. Thus, in practical situations it is relatively easy to select the parameters of soft and short inclusions ('gaskets') to suppress propagation of waves in a periodic plate in a given frequency band.

3. Propagation of axisymmetric waves in a cylindrical shell composed by a set of alternating elements

A classic theory of thin cylindrical shells [16] is adopted and the present analysis is restricted by the axisymmetric ('breathing') modes of vibrations. This choice is explained by the fact that wave propagation at high order modes ($m > 1$) even in a homogeneous shell is possible only by starting from a certain cut-on frequency, whereas a simplified theory may be used for analysis of wave propagation at a 'beam-type' mode ($m = 1$) in the mid-to-high frequency range. Therefore, the case $m = 0$ appears to be the most practical to apply a shell theory in analysis of stop bands phenomena. An infinitely long shell is composed by the set of periodically repeated elements of

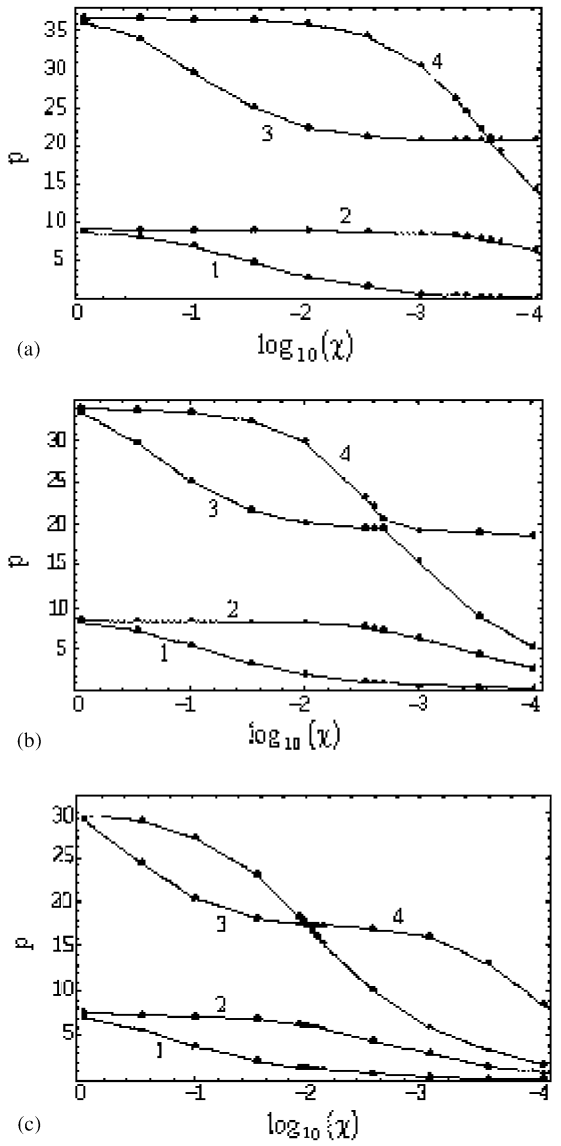

Fig. 3. The width of band gaps as a function of the stiffness ratio χ: (a) $\delta = 0.04$; (b) $\delta = 0.08$; (c) $\delta = 0.16$. Other parameters are $\alpha = 1$, $\beta = 1$, $\lambda = 100$.

two types as shown in Fig. 4. Each set of elements $(j = 1, 2)$ is specified by the following parameters: the thickness h_j, the radius R_j, the length l_j, Young's modulus E_j, the density ρ_j, and the Poisson coefficient v_j. Hereafter, it is assumed that $R_1 = R_2 = R$, and $v_1 = v_2 \equiv v = 0.3$. A stationary wave propagates at a circular frequency ω. It is convenient to introduce the non-dimensional parameters $\Omega_1 = \sqrt{(1 - v^2)\rho_1 R^2 \omega^2 / E_1}$, $\lambda_1 = l_1/R$, $\delta = l_2/l_1$, $\alpha = h_2/h_1$, $\beta = \rho_2/\rho_1$, $\chi = E_2/E_1$.

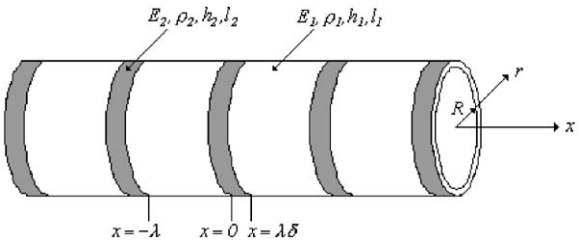

Fig. 4. A periodic cylindrical shell composed of continuous segments of two types.

Equations of dynamics of the elements of a shell are written for the axial (u) and the radial (w) displacements in the non-dimensional form ($u_j = u_j^{\dim}/R$, $w_j = w_j^{\dim}/R$, $j = 1, 2$, $x = x^{\dim}/R$) as

$$u_j'' + \nu w_j' + \frac{\rho_j E_1}{\rho_1 E_j}\Omega_1^2 u_j = 0, \tag{7a}$$

$$\nu u_j' + w_j + \frac{h_j^2}{12R^2} w_j^{(4)} - \frac{\rho_j}{\rho_1}\frac{E_1}{E_j}\Omega_1^2 w_j = 0, \quad j = 1, 2. \tag{7b}$$

A solution for this set of equations is sought in the form ($k_{nj} = k_{nj}^{\dim} R$)

$$w_j(x) = \sum_{n=1}^{6} A_{nj} \exp(\mathrm{i}k_{nj}x),$$

$$u_j(x) = \sum_{n=1}^{6} B_{nj} \exp(\mathrm{i}k_{nj}x), \quad j = 1, 2. \tag{8}$$

The wave numbers are found from the dispersion equations for each segment of a shell

$$\left(-k_j^2 + \frac{\rho_j}{\rho_1}\frac{E_1}{E_j}\Omega_1^2\right)\left(1 + \frac{h_j^2}{12R^2}k_j^4 - \frac{\rho_j}{\rho_1}\frac{E_1}{E_j}\Omega_1^2\right) + \nu^2 k_j^2 = 0, \quad j = 1, 2. \tag{9}$$

For each individual root of these equations, a modal coefficient is found, which defines the ratio between amplitudes of the axial and the radial displacements,

$$\frac{B_{nj}}{A_{nj}} = \frac{\mathrm{i}\nu k_{nj}}{k_{nj}^2 - \frac{\rho_j}{\rho_1}\frac{E_1}{E_j}\Omega_1^2} \equiv \mathrm{i}\frac{1 + \frac{h_j^2}{12R^2}k_{nj}^4 - \frac{\rho_j}{\rho_1}\frac{E_1}{E_j}\Omega_1^2}{\nu k_{nj}}, \quad j = 1, 2. \tag{10}$$

There are 12 unknown modal amplitudes in Eq. (8). They are uniquely defined by the continuity and the periodicity conditions, formulated (see Ref. [16] for details) for the axial displacements u, the axial forces $T \equiv (Eh/(1-\nu^2))(u' + \nu w)$, the radial displacements w, the slopes w', the bending moments $M \equiv (Eh^3/(12(1-\nu^2)))w''$ and the transverse forces $Q \equiv (Eh^3/(12(1-\nu^2)))w'''$ at junction points $x = 0$ and $x = \lambda_1\delta$ (see Fig. 4).

$$u_1(0) = u_2(0), \quad u_1'(0) + vw_1(0) = \chi\alpha[u_2'(0) + vw_2(0)],$$
$$w_1(0) = w_2(0), \quad w_1'(0) = w_2'(0),$$
$$w_1''(0) = \chi\alpha^3 w_2''(0), \quad w_1'''(0) = \chi\alpha^3 w_2'''(0), \tag{11a}$$

$$u_1(\lambda_1\delta) = u_2(\lambda_1\delta), \quad u_1'(\lambda_1\delta) + vw_1(\lambda_1\delta) = \chi\alpha[u_2'(\lambda_1\delta) + vw_2(\lambda_1\delta)],$$
$$w_1(\lambda_1\delta) = w_2(\lambda_1\delta), \quad w_1'(\lambda_1\delta) = w_2'(\lambda_1\delta),$$
$$w_1''(\lambda_1\delta) = \chi\alpha^3 w_2''(\lambda_1\delta), \quad w_1'''(\lambda_1\delta) = \chi\alpha^3 w_2'''(\lambda_1\delta). \tag{11b}$$

The same continuity conditions should also hold at all other junction points, $x = n(\delta + 1)\lambda_1$, $n = 0, 1, 2, \ldots$.

Floquet theory is applied to formulate the periodicity conditions

$$w_1(\delta\lambda_1) = w_1(-\lambda_1)\exp(\mathrm{i}\mathrm{K}_B),$$
$$w_1'(\delta\lambda_1) = w_1'(-\lambda_1)\exp(\mathrm{i}\mathrm{K}_B),$$
$$w_1''(\delta\lambda_1) = w_1''(-\lambda_1)\exp(\mathrm{i}\mathrm{K}_B),$$
$$w_1'''(\delta\lambda_1) = w_1'''(-\lambda_1)\exp(\mathrm{i}\mathrm{K}_B),$$
$$u_1(\delta\lambda_1) = u_1(-\lambda_1)\exp(\mathrm{i}\mathrm{K}_B),$$
$$u_1'(\delta\lambda_1) = u_1'(-\lambda_1)\exp(\mathrm{i}\mathrm{K}_B). \tag{12}$$

These conditions are substituted in Eqs. (11b) and the system of 12 homogeneous equations with respect to the two sets of modal amplitudes A_{nj}, $n = 1, 2, \ldots, 6$, $j = 1, 2$ is formulated. This system has a non-trivial solution when its determinant vanishes. As discussed, for any given frequency parameter Ω_1, this condition yields a transcendent equation (6) with respect to the Bloch parameter K_B. Unlike the previous case, the characteristic equation (6) for alternating cylindrical segments cannot be explicitly formulated as $\Omega_1(\mathrm{K}_B) = 0$. Then only the direct problem may be formulated: to find a value of the Bloch parameter K_B in the interval $0 < \mathrm{K}_B < \pi$ for a given Ω_1 from the original equation (6) and therefore to plot branches $\mathrm{K}_B(\Omega_1)$ one by one.

In Fig. 5, a set of characteristic curves $D(\Omega_1, \mathrm{K}_B) = 0$ (displayed as $\Omega_1(\mathrm{K}_B)$ for convenience) is presented for a cylindrical shell composed of the set of alternating elements. The lower and the upper parts of the graph are shown in Fig. 5a and b, respectively. In the case of a periodic plate, the band gaps are composed of the 'jumps' between the 'growing' and 'decaying' characteristic curves in an alternating sequence (see Fig. 2). Here this rule is applied only to the second and the third band gaps (a 'ladder' sequence of curves 2, 3 and 4, Fig. 5b), whereas the first one is actually defined as a distance between the highest and the lowest points of 'growing' branches 1 and 2 in Fig. 3a. This phenomenon has an elementary explanation, which will be provided later in this section. The 'density' of distribution of characteristic curves is very high in a high-frequency range ($\Omega_1 \sim 1$) and branches $\Omega_1(\mathrm{K}_B)$ are located in very narrow pass bands separated by equally narrow stop bands, as is seen from comparison of frequency parameter scaling in Fig. 5a and b. Thus, from the view point of possible engineering applications, it is relevant to explore the location of the first and the second band gaps only, whereas in a high-frequency range one may roughly assume the absence of stop bands.

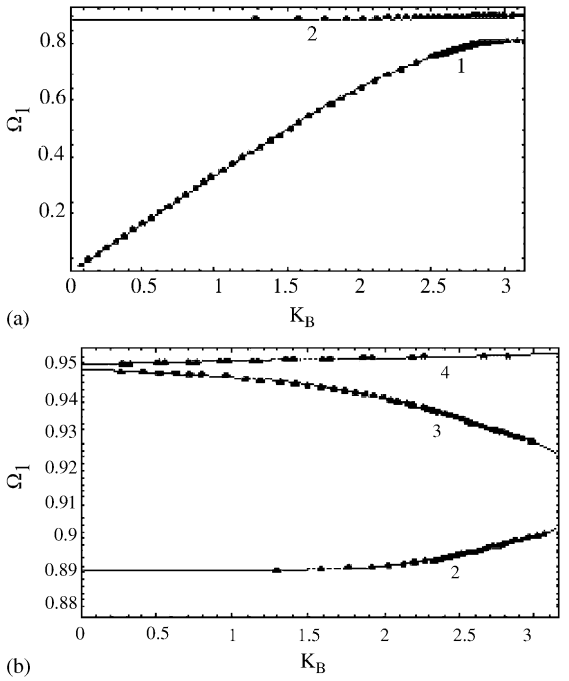

Fig. 5. Characteristic curves and band gaps in a periodic shell ($\nu = 0.3, h_1/R = 0.01$, $\alpha = 1$, $\beta = 1$, $\lambda_1 = 2$, $\delta = 0.01$, $\chi = 0.01$) without fluid loading: (a) low-frequency range; (b) high-frequency range.

For a slightly thinner shell, location of band gaps is shown in Fig. 6a. Similarly to the previous case, the first one is formed as a 'jump' between growing curves 1 and 2, whereas the second one is composed of a 'jump' between the 'growing' and 'decaying' characteristic curves. In Fig. 6b, the dependence of $\mathrm{Min}|\mathrm{Im}\,\mathrm{K}_B|$ on a frequency parameter is plotted in the first and the second stop bands. Curve 2 is similar to its counterparts for a periodic plate (see Fig. 2), whereas in the first band gap the wave propagation is suppressed very heavily almost at the upper threshold frequency of the second pass band. Actually, curve 1a (a continuation of curve 1 in Fig. 6a) is intersected very close to this threshold frequency by another branch 1b, which is sketched in Fig. 6b as a straight almost horizontal line (similar to the extreme upper part of curve 2).

The location of band gaps in the frequency domain is summarized in Table 1 for several values of thickness ratio. All other parameters are fixed as $\nu = 0.3$, $\alpha = 1$, $\beta = 1$, $\lambda_1 = 2$, $\delta = 0.01$, $\chi = 0.01$. To explain the structure of these band gaps it is expedient to note that axisymmetric motions of a cylindrical shell actually comprise longitudinal and flexural vibrations coupled due to Poisson effect. Indeed, if $\nu = 0$, Eqs. (7a) and (7b) are decoupled. Then a problem in longitudinal vibrations is formulated as

$$u_j'' + \frac{\rho_j}{\rho_1}\frac{E_1}{E_j}\Omega_1^2 u_j = 0. \tag{13}$$

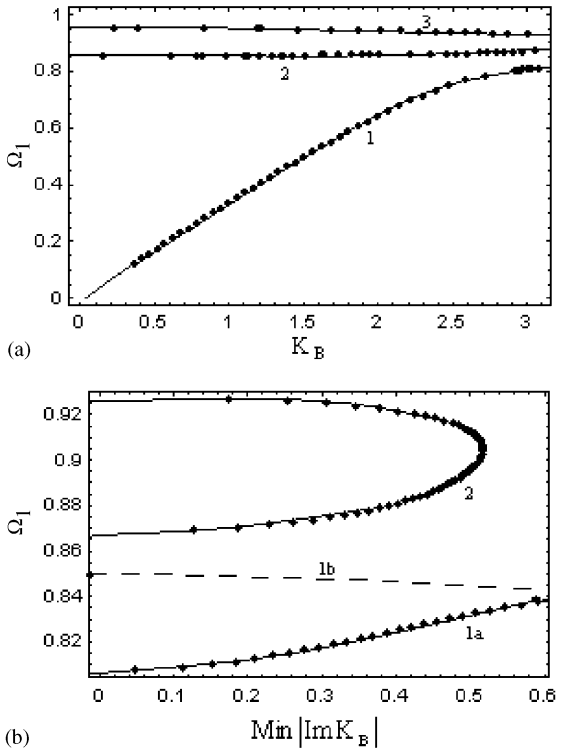

Fig. 6. Characteristic curves and band gaps in a periodic shell ($\nu = 0.3$, $h_1/R = 0.005$, $\alpha = 1$, $\beta = 1$, $\lambda_1 = 2$, $\delta = 0.01$, $\chi = 0.01$) without fluid loading: (a) purely real branches; (b) purely imaginary branches.

Table 1
The band gaps in a cylindrical shell without fluid loading

h_1/R	The first band gap	The second band gap	The third band gap
0.002	$0.767 < \Omega_1 < 0.778$	$0.825 < \Omega_1 < 0.928$	$0.949 < \Omega_1 < 0.951$
0.005	$0.809 < \Omega_1 < 0.853$	$0.869 < \Omega_1 < 0.928$	$0.948 < \Omega_1 < 0.949$
0.010	$0.811 < \Omega_1 < 0.891$	$0.901 < \Omega_1 < 0.928$	—
0.050	$0.815 < \Omega_1 < 0.927$	$0.933 < \Omega_1 < 0.934$	—

This equation should be solved with the continuity and the periodicity conditions at junction points $x = 0$, $x = \lambda_1\delta$:

$$u_1(0) = u_2(0), \quad u_1'(0) = \chi\alpha u_2'(0),$$
$$u_1(\lambda_1\delta) = u_2(\lambda_1\delta), \quad u_1'(\lambda_1\delta) = \chi\alpha u_2'(\lambda_1\delta),$$
$$u_1(\lambda_1\delta) = u_1(-\lambda_1)\exp(\mathrm{i}K_B), \quad u_1'(\lambda_1\delta) = u_1'(-\lambda_1)\exp(\mathrm{i}K_B).$$

Solution of this problem does not depend on the parameter h_1/R. The first branch of characteristic curve is presented by curve 1 in Fig. 7a. The second branch is located at a much higher value of Ω_1 (approximately at $\Omega_1 \approx 1.6$) and is not displayed here. Curve 2 is reproduced here from Fig. 5a for a shell with $h_1/R = 0.01$ (actually, this curve has almost the same shape for

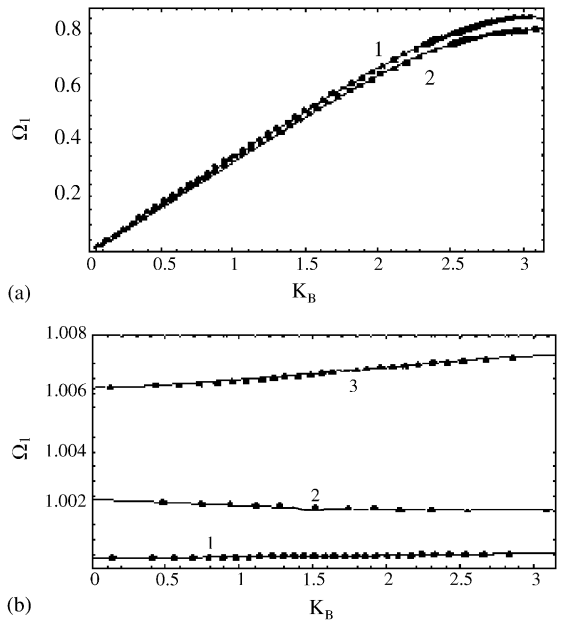

Fig. 7. Characteristic curves and band gaps in a periodic shell with $h_1/R = 0.01$, $\alpha = 1$, $\beta = 1$, $\lambda_1 = 2$, $\delta = 0.01$, $\chi = 0.01$. Comparison with an elementary theory of (a) longitudinal waves and (b) flexural waves.

all other magnitudes of the parameter h_1/R listed in Table 1). As seen, there is a very good agreement between curves 1 and 2 (the ordinate of the upper point predicted in a rod theory exceeds the prediction of a shell theory only in 5%) and it proves that the propagating wave, which exists in a periodic structure at low frequencies, is a wave of the dominantly longitudinal deformation of a cylindrical shell.

A problem in purely flexural vibrations is formulated as

$$w_j + \frac{h_j^2}{12R^2} w_j^{(4)} - \frac{\rho_j}{\rho_1}\frac{E_1}{E_j}\Omega_1^2 w_j = 0. \tag{14}$$

The continuity conditions at junction points $x = 0$, $x = \lambda_1\delta$ are

$$\begin{aligned}
&w_1(0) = w_2(0), \quad w_1'(0) = w_2'(0),\\
&w_1''(0) = \chi\alpha^3 w_2''(0), \quad w_1'''(0) = \chi\alpha^3 w_2'''(0),\\
&w_1(\lambda_1\delta) = w_2(\lambda_1\delta), \quad w_1'(\lambda_1\delta) = w_2'(\lambda_1\delta),\\
&w_1''(\lambda_1\delta) = \chi\alpha^3 w_2''(\lambda_1\delta), \quad w_1'''(\lambda_1\delta) = \chi\alpha^3 w_2'''(\lambda_1\delta).
\end{aligned}$$

The periodicity conditions at $x = \lambda_1\delta$ are

$$\begin{aligned}
&w_1(\delta\lambda_1) = w_1(-\lambda_1)\exp(\mathrm{i}K_B),\\
&w_1'(\delta\lambda_1) = w_1'(-\lambda_1)\exp(\mathrm{i}K_B),\\
&w_1''(\delta\lambda_1) = w_1''(-\lambda_1)\exp(\mathrm{i}K_B),\\
&w_1'''(\delta\lambda_1) = w_1'''(-\lambda_1)\exp(\mathrm{i}K_B).
\end{aligned}$$

This problem formulation is, in effect, identical to the problem formulation for a beam lying on a Winckler elastic foundation [17]. Characteristic curves 1–3 displayed in Fig. 7b are obtained in this reduced formulation of a problem in flexural vibrations. As is well known, flexural waves may propagate in an infinitely long uniform beam lying on an elastic foundation only above a cut on frequency. Here it is clearly observed that the frequency parameter should exceed the cut on frequency of both segments (i.e. $\Omega_1 > 1$). The characteristic curves obtained by solving this auxiliary problem are closely spaced. Each of these curves should be referred to its counterpart in Fig. 5b, where three branches are presented for $h_1/R = 0.01$, $\nu = 0.3$. Comparison of the graphs in Figs. 5b and 7b (note the difference in scales for frequency parameter Ω_1, which makes it impossible to display them in the same graph) shows that propagation of axisymmetric flexural waves in a cylindrical shell composed of a set of alternating elements quantitatively cannot be described in a reduced formulation. However, qualitatively the structure of characteristic curves is adequately explained. Specifically, the lower part of characteristic curves $\Omega_1(\mathrm{K}_B)$ shown in Figs. 5a and 6a is indeed related to propagation of the longitudinal wave and it is not influenced by the parameter of a shell thickness. The second characteristic curve $\Omega_1(\mathrm{K}_B)$ in a cylindrical shell (which also grows from the left to the right) is actually the first one related to propagation of a flexural wave above its cut on frequency (see curves 2 in Figs. 5a and b and in Fig. 6a). Location of this branch is affected by the shell thickness parameter. For a thin shell ($h_1/R = 0.002$), this branch approaches the 'longitudinal' branch, whereas for a relatively thick shell ($h_1/R = 0.05$), it lies well above the displayed frequency parameter range.

4. Propagation of flexural waves in a fluid-loaded plate composed by a set of alternating elements

An infinitely long plate is extended in x direction ($-\infty < x < \infty$) and made up of the set of alternating elements of two types as described in Section 2. This structure is loaded by the layer of a homogeneous acoustic medium of the uniform depth H located below the plate ($-\infty < x < \infty$, $-H < z < 0$). All parameters of the plate elements are introduced in Section 2 and here the same notations are used. The fluid is characterized by the density ρ_{fl} and the sound speed c_{fl}. Propagation of a stationary wave in this elasto-acoustic system at a circular frequency ω is considered. The dynamics of a fluid-loaded plate are then governed by equations ($p_j = 12(1-\nu^2)p_j^{\dim}/E_1$, $j = 1, 2$)

$$w_1^{(4)} - 12\Omega^2 w_1 = p_1, \quad -\lambda + n\lambda(1+\delta) < x < n\lambda(1+\delta), \quad n = 0, 1, 2, \ldots, \tag{15a}$$

$$w_2^{(4)} - 12\Omega^2\alpha^{-2}\beta\chi^{-1}w_2 = p_2\chi^{-1}, \quad n\lambda(1+\delta) < x < \lambda\delta + n\lambda(1+\delta), \quad n = 0, 1, 2, \ldots\ . \tag{15b}$$

Helmholtz equation is held in the whole volume occupied by a fluid. Although the fluid's properties are the same in the whole volume, it is convenient to introduce two velocity potentials φ_1 and φ_2, which describe wave motions in alternating fluid volumes contacted by the plate elements of each type. Non-dimensional velocity potentials are introduced as $\varphi_j = \varphi_j^{\dim}/h_1 c$, $j = 1, 2$ (here $c = \sqrt{E_1/\rho_1}$) and a Helmholtz equation is formulated for each

of them:

$$\frac{\partial^2\varphi_j}{\partial x^2}+\frac{\partial^2\varphi_j}{\partial z^2}+\left(\frac{\omega h_1}{c_{fl}}\right)^2\varphi_j=0,\quad j=1,2. \tag{16}$$

The non-dimensional acoustic pressure is expressed via the velocity potential as

$$p_j=12(1-\nu^2)\mathrm{i}\frac{\rho_{fl}}{\rho_1}\frac{\omega h_1}{c}\varphi_j. \tag{17}$$

The boundary condition is formulated at the rigid baffle ($z=-H/h_1=-\eta$) as

$$\frac{\partial\varphi_j}{\partial z}=0,\quad j=1,2. \tag{18}$$

At the surface of a plate the boundary condition is

$$\frac{\partial\varphi_1}{\partial z}=-\mathrm{i}\frac{\omega h_1}{c}w_1,\quad n(1+\delta)\lambda<x<\lambda+n(1+\delta)\lambda, \tag{19a}$$

$$\frac{\partial\varphi_2}{\partial z}=-\mathrm{i}\frac{\omega h_1}{c}w_2,\quad \lambda+n(1+\delta)\lambda<x<\lambda(1+\delta)+n(1+\delta)\lambda. \tag{19b}$$

A periodic structure is considered, so that (similarly to the case of the absence of a fluid) continuity conditions (4) are introduced at the junction points between plate elements of different types. However, now the alternating elastic elements are fluid- loaded and it is necessary to match also the fluid fields (velocity potentials φ_1, φ_2 and their gradients, which describe wave motion in a fluid) at the interfaces between the volumes contacted by plate elements of different properties. These conditions are formulated for a pressure and for an axial velocity at $x=n(1+\delta)\lambda$, $x=\lambda+n(1+\delta)\lambda$ along the continuous fluid interface $-\eta<z<0$

$$\varphi_1(x,z)=\varphi_2(x,z), \tag{20a}$$

$$\frac{\partial\varphi_1(x,z)}{\partial x}=\frac{\partial\varphi_2(x,z)}{\partial x}. \tag{20b}$$

Apparently, the first derivatives of velocity potentials in the transverse direction z are matched automatically inasmuch the condition in Eq. (20a) holds true.

Velocity potentials should also obey the periodicity conditions

$$\begin{aligned}&\varphi_1(x,z)|_{x=\delta\lambda}=\varphi_1(x,z)|_{x=-\lambda}\exp(\mathrm{i}K_B),\\ &\left.\frac{\partial\varphi_1(x,z)}{\partial x}\right|_{x=\delta\lambda}=\left.\frac{\partial\varphi_1(x,z)}{\partial x}\right|_{x=-\lambda}\exp(\mathrm{i}K_B).\end{aligned} \tag{21}$$

A solution of the homogeneous problem (15–19) for each elasto-acoustic element is formulated as

$$w_j(x)=A_j\exp(\mathrm{i}k_jx), \tag{22a}$$

$$\varphi_j(x,z)=\Phi_j(z)\exp(\mathrm{i}k_jx). \tag{22b}$$

Substitution of Eqs. (22a, b) to Eqs. (15–19) and standard transformations (see, for example, the derivation for a sandwich plate with heavy fluid loading in Ref. [18]) give the following transcendent dispersion equations defining wave numbers ($\Gamma_1=\sqrt{k_1^2-(c/c_{fl})^2\Omega^2}$,

$\Gamma_2 = \sqrt{k_2^2 - (c/c_{fl})^2\Omega^2}$) for each fluid-loaded plate element

$$k_1^4 - 12\Omega^2 - 12\Omega^2 \frac{\rho_{fl}}{\rho_1}\frac{1}{\Gamma_1}\frac{\cosh(\Gamma_1\eta)}{\sinh(\Gamma_1\eta)} = 0, \tag{23a}$$

$$k_2^4 - 12\Omega^2\alpha^{-2}\beta\chi^{-1} - 12\Omega^2\alpha^{-3}\frac{\rho_{fl}}{\rho_1}\chi^{-1}\frac{1}{\Gamma_2}\frac{\cosh(\Gamma_2\eta)}{\sinh(\Gamma_2\eta)} = 0. \tag{23b}$$

Unlike their counterparts (1a, b), these equations have an infinite number of roots. Straightforward transformations in the two limit cases: (a) $\rho_{fl}/\rho_1 \to 0$ (the absence of a fluid); (b) $\rho_{fl}c_{fl}^2/E_1 \to 0$ (an absolutely rigid plate) result in dispersion equations for a simple plate and for an acoustic layer between the rigid walls, respectively. A solution for each segment of a plate with fluid loading is sought in the form of a modal decomposition of displacements and velocity potentials with a finite number of terms retained as

$$w_j(x) = \sum_{n=1}^{N_j} A_{nj}\exp(\mathrm{i}k_{nj}x), \tag{24a}$$

$$\varphi_j(x) = -\mathrm{i}\frac{\omega h_1}{c}\sum_{n=1}^{N_j} A_{nj}\Phi_{nj}(z)\exp(\mathrm{i}k_{nj}x), \quad j = 1, 2. \tag{24b}$$

Eigenfunctions, which represent a distribution of velocity potential in transverse co-ordinate z for each individual wave number, are introduced in Eq. (24b) as

$$\Phi_{nj}(z) = \frac{\exp(2\Gamma_{nj}\eta + \Gamma_{nj}z) + \exp(-\Gamma_{nj}z)}{\Gamma_{nj}[\exp(2\Gamma_{nj}\eta) - 1]}. \tag{25}$$

Eqs. (24) present an exact solution for a fluid-loaded plate element as $N_j \to \infty$.

Since it is computationally difficult to find directly the complex-valued roots of transcendent equations (23a, b), some simple transformations outlined in Ref. [19] are made. Namely, each of these equations is multiplied by $\sinh(\Gamma_j\eta)$ and the functions $\Gamma_j\sinh(\Gamma_j\eta)$ and $\cosh(\Gamma_j\eta)$ are expanded into polynomials in $\Gamma_j^2 = k_j^2 - (c/c_{fl})^2\Omega^2$. Then dispersion equations are formulated in the polynomial form both in Ω^2 and in k_j^2 and their order is controlled by the number of terms retained in normal expansions of hyper-trigonometric functions of the argument Γ_j. It is a trivial task to find all roots of a polynomial equation of an arbitrary high order and it also does not present any difficulties to vary the number of terms in normal series and therefore to control convergence of roots of approximate dispersion equations. However, the transformation of the original dispersion equation to a polynomial form inevitably generates 'spurious' roots, which do not originate from the exact formulation of Eq. (23). Thus, all roots of the polynomial dispersion equations are separately supplied as an 'initial guess' to a numerical procedure of searching a root of the original transcendent dispersion equation and this procedure gives a set of 'genuine' roots—wave numbers, which are used in modal decomposition (Eq. (24)).

For a plate without fluid loading, the number of roots of dispersion equations (1a, b) is exactly the same as the number of conditions (4a, b) and the exact characteristic equation is derived to determine Bloch parameters in Section 2. In the case of a plate with fluid loading, additional continuous conditions (20a, b) are formulated for velocity potentials presented by a finite number of terms in expansions (24a, b). Then it is necessary to suggest some approximate procedure to

satisfy conditions (20a, b) in an average sense. Discussion of this issue with respect to formulation of Green's matrices for sandwich plates in contact with the layer of an acoustic medium is available, for example, in Ref. [18]. It should be pointed out that although dispersion equations (23a, b) have an infinite number of roots, in a low-frequency regime (which is most important from the practical point of view) the majority of these roots are purely imaginary. These roots describe evanescent waves, which are not involved in energy transportation. The Kirchhoff plate theory adopted here to describe structural dynamics is applicable only in a low and moderate frequency range. In these frequency ranges the dispersion equations have just one or two purely real roots and, therefore, only one or two waves may propagate in each elasto-acoustic element. Since the analysis of stationary dynamics of periodic fluid-loaded structures is aimed at detection of conditions for wave propagation, it is essential to retain all propagating waves in modal expansions (24a, b). Then 'fluid' continuity and periodicity conditions may be formulated in an approximate way by applying some condensation technique, such as, for example, the Galerkin method. Although conditions (20a, b) are approximated with better accuracy when the number of terms in modal expansions (24a, b) is increased, qualitatively correct results may be obtained as soon as all propagating waves are retained in the analysis [2].

As is seen from Eqs. (24a, b), each normal wave in a coupled elasto-acoustic element is characterized by an eigenfunction, which presents a distribution of velocity potential across the layer of a fluid in the z direction. Then Galerkin orthogonalisation may conveniently be applied to formulate continuity conditions (20a, b) in the averaged sense at $x = n(1+\delta)\lambda$, $x = \lambda + n(1+\delta)\lambda$:

$$\int_{-\eta}^{0} [\varphi_1(x,z) - \varphi_2(x,z)]\phi_j(x,z)\,\mathrm{d}z = 0, \tag{26a}$$

$$\int_{-\eta}^{0} \left[\frac{\partial\varphi_1(x,z)}{\partial x} - \frac{\partial\varphi_2(x,z)}{\partial x}\right]\phi_j(x,z)\,\mathrm{d}z = 0. \tag{26b}$$

The natural choice of 'weight' functions $\phi_j(x,z)$ in Eqs. (26) is of course a set of eigenfunctions (25). However, two issues should be addressed with respect to this averaging procedure. Firstly, the structural continuity conditions (4) must be satisfied besides these ones and secondly, there are two sets of functions $\Phi_{nj}(z)$, $n = 1, 2$.

As has been discussed in Ref. [18], the roots of dispersion equations (23) may be identified as the 'structure-originated' and the 'fluid-originated' ones. The number of the former roots is eight (the two sets of four roots each), whereas the number of the latter is in fact controlled by the number of terms retained in modal expansions (24) and therefore varies. Respectively, eight 'structural' conditions (4) should be satisfied, whereas continuous 'fluid' conditions (26) may be averaged many times as many 'fluid-originated' roots and 'fluid-originated' eigenfunctions (25) are found.

In all computations reported in the paper, the same number of modes is retained in modal expansions for both coupled elasto-acoustic elements, e.g., $N_1 = N_2 = 2N_0$. The roots of dispersion equations are always structured in pairs ($\pm$K), so the number of terms, retained in expansions (24) is always even, $2N_0$. The 'global' system of governing equations contains $N_1 + N_2 = 4N_0$ modal amplitudes.

Once eight structural continuity and periodicity conditions (4) are formulated, it is necessary to add $4N_0 - 8$ conditions (26) to complete the system of governing equations. As is seen from Eq. (25), the eigenfunctions $\Phi_{nj}(z)$ related to each pair of roots $\pm$K are identical. There are N_0

different eigenfunctions for each element. Two of them (in each set) are 'structure-originated' and should not be used in setting up additional equations. Thus, the set of $N_0 - 2$ 'weight' functions is available to average four continuity conditions, i.e., the two sets of Eqs. (26a, b) at the points $x = n(1+\delta)\lambda$ and $x = \lambda + n(1+\delta)\lambda$. Apparently, it gives $4N_0 - 8$ algebraic equations, which is precisely as many as necessary. The 'weight' functions may be taken as eigenfunctions for any of two elasto-acoustic elements. In all computations reported in this paper, the system of linear algebraic equations is formulated and solved twice (with the use of both sets of eigenfunctions in turn) and there is no difference in results. This fact has an elementary physical interpretation. In the problem formulation, discontinuity is introduced by a jump in the structural parameters and structure-originated modes $\Phi_{nj}(z)$, $n = 1, 2, \ldots, 8, j = 1, 2$ are substantially different in the two sets of coupled elasto-acoustic elements, whereas fluid-originated modes $\Phi_{nj}(z)$, $n = 5, \ldots, 2N_0$ are almost identical. If the roots of dispersion equation for each element are ranged by growth in magnitude, then the difference between the 'counterpart' modes in the two sets tends to zero.

To illustrate the wave propagation phenomena in a structure with heavy fluid loading, consider a plate with the following parameters: $\alpha = 1$, $\beta = 1$, $\lambda = 200$, $\delta = 0.04$, $\chi = 0.01$. Fluid is specified by the density ratio $\rho = \rho_{fl}/\rho_1 = 0.128$, the sound speed ratio $\bar{c} = c_{fl}/c = 0.307$ (these two parameters are typical for vibrations of a steel plate in water) and also by the depth ratio η.

Before addressing wave propagation in a periodic fluid loaded structure, it is relevant to discuss dispersion diagrams for each of its elasto-acoustic elements. In Figs. 8 and 9, dispersion curves $k(p)$ are plotted at $\eta = 100$ for the 'stiff' and 'soft' elements, respectively. Curves 1, 2 in Figs. 8a and 9a present a dependence of the purely real wave numbers (they specify free propagating waves) upon the frequency parameter. Respectively, curves 3, 4, 5, 6 in Figs. 8a,b and 9a,b present

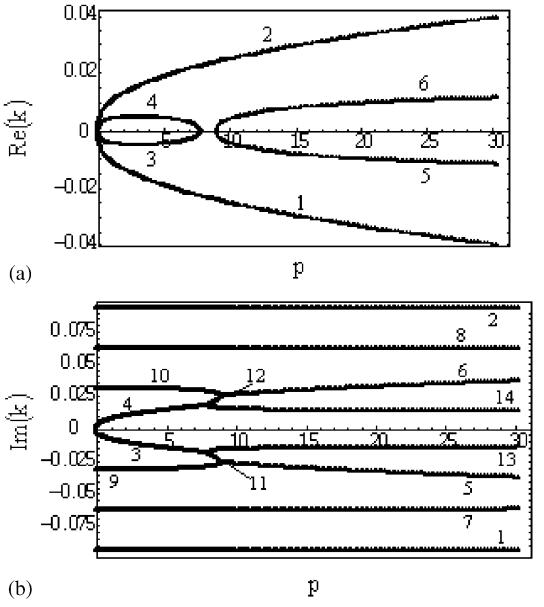

Fig. 8. Dispersion curves for a 'stiff' element of a periodic plate with heavy fluid loading. (a) Purely real wave numbers and the real parts of the complex wave numbers; (b) purely imaginary wave numbers and the imaginary parts of the complex wave numbers.

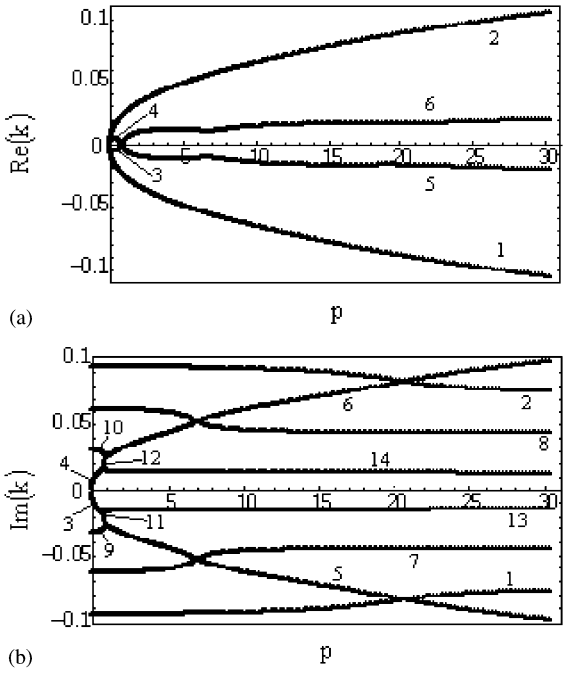

Fig. 9. Dispersion curves for a 'soft' element of a periodic plate with heavy fluid loading; (a) purely real wave numbers and the real parts of the complex wave numbers; (b) purely imaginary wave numbers and the imaginary parts of the complex wave numbers.

the complex-valued wave numbers. Finally, curves 1,2, 7–14 in Figs. 8b and 9b display a dependence of purely imaginary roots on frequency parameter. The behaviour of dispersion curves is similar to the case of a fluid-loaded sandwich plate studied in Ref. [18]. In Fig. 10a and b, a zoomed picture from Fig. 9a and b is shown and it is seen that the location of dispersion curve in the frequency range $0.75 < p < 0.925$ for the 'soft' segment is qualitatively the same as for the 'stiff' one in the range $7.0 < p < 9.0$. It should be pointed out that the magnitudes of the 'fluid-originated' roots in both elasto-acoustic elements are almost the same that supports the above discussion of the choice of weight functions in the averaged equations (26). In all computations, 10 normal modes for each element are retained, $N_1 = N_2 = 2N_0 = 10$. As is seen, there is only one propagating wave in each elasto-acoustic element for the whole frequency range considered (more precisely, there are two waves with the same wave number, which propagate in opposite directions). It is elementary to show that this free wave is a 'structure-originating' one. The 'fluid-originating' modes are cut-on at much higher frequencies.

The free wave propagation in a periodic plate with fluid loading is compared with the wave propagation in a 'simple' plate in Figs. 11 and 12. Characteristic curves $p(\mathrm{K}_B)$ in Fig. 11a and b are plotted by curves 1a, b for a plate without fluid loading, by curves 2a, b for a plate loaded by the fluid layer of a depth $\eta = 100$ and by curves 3a, b in a case, when $\eta = 20$. The first and the second band gaps are presented in Table 2. As is seen, heavy fluid loading produces a very significant influence on the location and the width of both band gaps. All characteristic curves for a fluid loaded plate are pulled significantly downwards from their counterparts for a plate without

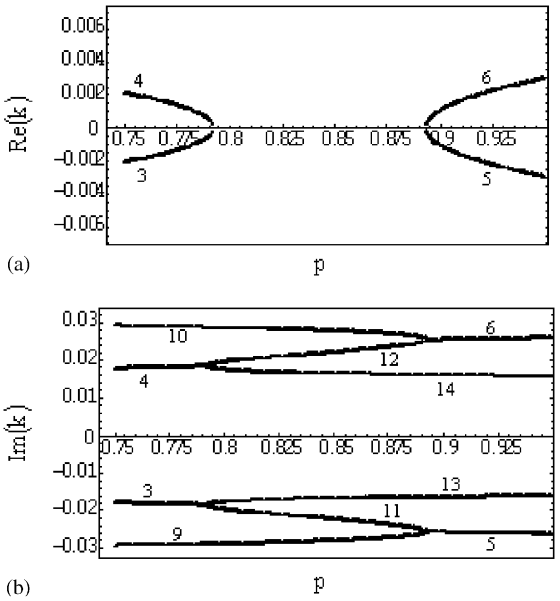

Fig. 10. Zooming of Fig. 9a and b.

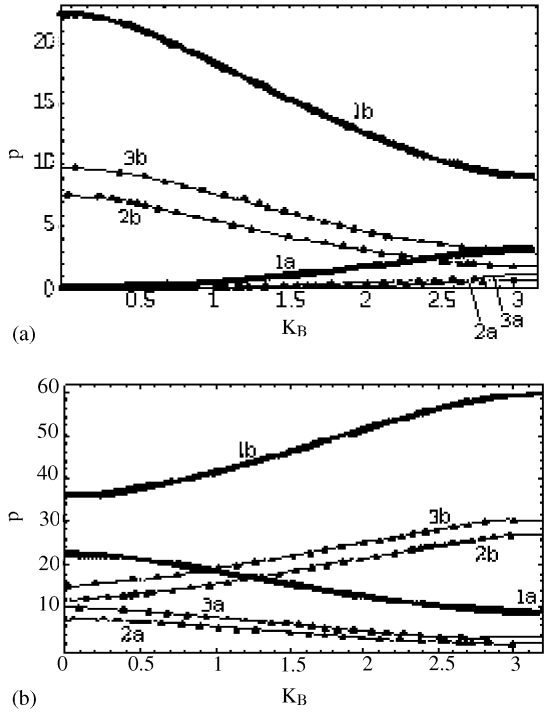

Fig. 11. Characteristic curves and band gaps in a periodic plate with fluid loading: $\alpha = 1$, $\beta = 1$, $\lambda = 200$, $\delta = 0.04$, $\chi = 0.01$, $\rho = 0.128$, $\bar{c} = 0.307$.

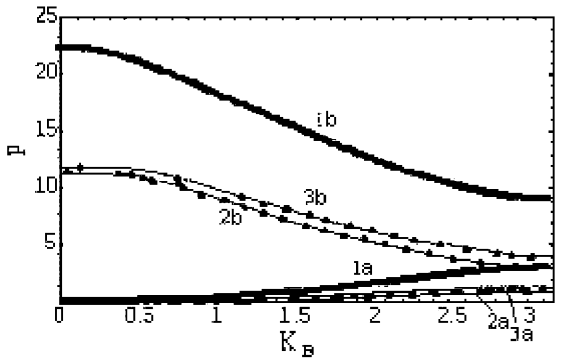

Fig. 12. Characteristic curves and band gaps in a periodic plate with fluid loading: $\alpha = 1$, $\beta = 1$, $\lambda = 100$, $\delta = 0.04$, $\chi = 0.01$, $\rho = 0.128$, $\bar{c} = 0.307$.

Table 2
The band gaps in a plate with fluid loading

	The first band gap	The second band gap
Empty	$2.85 < p < 9.05$	$22.41 < p < 35.82$
$\eta = 20$	$0.56 < p < 1.69$	$7.58 < p < 12.14$
$\eta = 100$	$0.81 < p < 3.01$	$9.78 < p < 15.17$

fluid loading, so that both band gaps are shifted towards lower frequencies. In addition, the width of band gaps is markedly narrowed due to the presence of a fluid. Similar conclusions may be drawn from the graphs, shown in Fig. 12, where the first and the second characteristic curves are plotted for a thicker plate (the notations are the same as is Fig. 11). Qualitatively the influence of fluid loading is similar in both these cases, but in the latter case the difference between characteristic curves plotted for $\eta = 100$ and 20 is less profound.

5. Propagation of axisymmetric waves in a fluid-filled cylindrical shell composed by a set of alternating elements

Consider an infinitely long shell, which is composed by the set of periodically repeated elements of two types as discussed in Section 3. This shell is filled by an acoustic medium, specified by its density ρ_{fl} and sound speed c_{fl}. A stationary wave at a circular frequency ω propagates in such a fluid-loaded shell. Fluid loading is defined by parameters $\rho = \rho_{fl}/\rho_1$ and $\bar{c} = c_{fl}/c_1$, which are introduced in addition to the non-dimensional parameters used in Section 3. Equations of dynamics of the elements of a shell in the non-dimensional form ($u_j = u_j^{\dim}/R$, $w_j = w_j^{\dim}/R$, $p_j = p_j^{\dim}/E_1$, $j = 1, 2$, $x = x^{\dim}/R$) are

$$u_j'' + \nu w_j' + \frac{\rho_j}{\rho_1}\frac{E_1}{E_j}\Omega_1^2 u_j = 0, \tag{27a}$$

$$\nu u_j' + w_j + \frac{h_j^2}{12R^2} w_j^{(4)} - \frac{\rho_j}{\rho_1}\frac{E_1}{E_j}\Omega_1^2 w_j = (1-\nu^2)\frac{R}{h_j} p_j, \quad j = 1,2. \tag{27b}$$

As in the case of a fluid-loaded plate, non-dimensional velocity potentials are introduced for each element as $\varphi_j = \varphi_j^{\dim}/(Rc_1)$, $j = 1,2$ ($c_1 = \sqrt{E_1/(\rho_1(1-\nu^2))}$) and a Helmholtz equation is formulated in cylindrical co-ordinates

$$\frac{\partial^2\varphi_j}{\partial x^2} + \frac{\partial^2\varphi_j}{\partial r^2} + \frac{1}{r}\frac{\partial\varphi_j}{\partial r^2} + \left(\frac{\omega R}{c_{fl}}\right)^2 \varphi_j = 0. \tag{28}$$

The non-dimensional acoustic pressure is expressed via velocity potential as

$$p_j = \mathrm{i}\frac{\rho_{fl}}{\rho}\frac{\omega R}{c_1}\varphi_j. \tag{29}$$

The velocity potentials must be bounded at the axis, e.g., $|\varphi_j(x,r)| < \infty$ as $r \to 0$. At the surface of a shell the boundary condition is

$$\frac{\partial\varphi_1}{\partial z} = -\mathrm{i}\frac{\omega R}{c_1} w_1, \quad n(1+\delta)\lambda_1 < x < \lambda_1 + n(1+\delta)\lambda_1, \tag{30a}$$

$$\frac{\partial\varphi_2}{\partial z} = -\mathrm{i}\frac{\omega R}{c_1} w_2, \quad \lambda_1 + n(1+\delta)\lambda_1 < x < \lambda_1(1+\delta) + n(1+\delta)\lambda_1. \tag{30b}$$

Exactly as in the case of a plate with heavy fluid loading, the continuity and periodicity conditions for a fluid-loaded shell consist of two parts. The first one concerns 'structural' conditions, which are formulated as Eqs. (11–12). The 'fluid' conditions are exactly the same as in the case of a plate. They are formulated as Eqs. (20–21) and should be held at $x = n(1+\delta)\lambda_1$, $x = \lambda_1 + n(1+\delta)\lambda_1$ along the continuous fluid interface $0 < r < 1$.

Thus, similar to the case of the absence of a fluid, a solution of the homogeneous problem (27)–(30) for each elasto-acoustic element is formulated as

$$w_j(x) = A_j \exp(\mathrm{i}k_j x), \tag{31a}$$

$$u_j(x) = B_j \exp(\mathrm{i}k_j x), \tag{31b}$$

$$\varphi_j(x) = \Phi_j(r)\exp(\mathrm{i}k_j x). \tag{31c}$$

The wave numbers are found from dispersion equations for each segment of a fluid-filled shell ($\mathrm{K}_1 = \sqrt{(c_1/c_{fl})^2\Omega_1^2 - k_1^2}$, $\mathrm{K}_2 = \sqrt{(c_1/c_{fl})^2\Omega_1^2 - k_2^2}$):

$$\left(-k_j^2 + \frac{\rho_j}{\rho_1}\frac{E_1}{E_j}\Omega_1^2\right)\left(1 + \frac{h_j^2}{12R^2}k_j^4 - \frac{\rho_j}{\rho_1}\frac{E_1}{E_j}\Omega_1^2\right) + \nu^2 k_j^2 + \frac{\rho_{fl}}{\rho_1}\Omega_1^2\frac{R}{h_j}\frac{J_0(\mathrm{K}_j)}{\mathrm{K}_j J_1(\mathrm{K}_j)}\left(-k_j^2 + \frac{\rho_j}{\rho_1}\frac{E_1}{E_j}\Omega_1^2\right) = 0, \quad j = 1,2. \tag{32}$$

These equations have infinitely many roots and the modal decomposition of displacements and velocity potentials is formulated as

$$w_j(x) = \sum_{n=1}^{N_j} A_{nj}\exp(\mathrm{i}k_{nj}x), \tag{33a}$$

$$u_j(x) = \mathrm{i}v \sum_{n=1}^{N_j} k_{nj} \left(k_{nj}^2 - \frac{\rho_j}{\rho_1} \frac{E_1}{E_j} \Omega_1^2 \right)^{-1} A_{nj} \exp(\mathrm{i}k_{nj}x), \tag{33b}$$

$$\varphi_j(x,r) = \mathrm{i} \frac{\omega R}{c_1} \sum_{n=1}^{N_j} A_{nj} \frac{J_0(\mathrm{K}_{nj}r)}{\mathrm{K}_{nj}J_1(\mathrm{K}_{nj})} \exp(\mathrm{i}k_{nj}x). \tag{33c}$$

Eqs. (33) present an exact solution for a fluid-loaded plate element as $N_j \to \infty$.

Simple transformations similar to those discussed in Section 4 are made to find several complex-valued roots of transcendent equations (32). Averaging of continuity and periodicity conditions is also performed for a fluid-filled shell exactly as for a plate with fluid loading. The number of the 'structure-originated' roots of dispersion equations (32) is 12 (the two sets of six roots each), whereas the number of the 'fluid- originated' ones is in fact controlled by the number of terms retained in modal expansions (33) and therefore varies. 12 'structural' conditions (11) should be satisfied, whereas continuous 'fluid' conditions (26) may be averaged as many times as the number of 'fluid-originated' roots and eigenfunctions found. In all computations reported in the paper, the same number of modes is retained in modal expansions for the both coupled elasto-acoustic elements, e.g., $N_1 = N_2 = 2N_0$. The 'global' system of governing equations contains $N_1 + N_2 = 4N_0$ modal amplitudes. It is necessary to set up $4N_0 - 12$ conditions (26) to complete the system of governing equations. Exactly as in the case of a plate with fluid loading, there are N_0 distinct eigenfunctions for each elasto-acoustic element. Three of them (in each set) are 'structure-originated' and should not be used in setting up additional equations. Thus, the set of $N_0 - 3$ 'weight' functions is available to average four continuity conditions. Apparently, it gives $4N_0 - 12$ algebraic equations, which is just as many as necessary. The 'weight' functions may be taken as eigenfunctions for any of two elasto-acoustic elements and all the discussion of this issue presented in Section 4 is equally applicable in this case.

To illustrate the wave propagation phenomena in a periodic structure with heavy fluid loading, consider a shell composed of two sets of alternating elements with the following parameters $h_1/R = 0.01$, $\alpha = 1$, $\beta = 1$, $\lambda_1 = 2$, $\delta = 0.01$, $\chi = 0.01$. Fluid is characterized by the density ratio $\rho = 0.128$ and the sound speed ratio $\bar{c} = 0.307$ (these two parameters are typical for vibrations of a steel shell filled by water).

In Fig. 13, dispersion curves $k(\Omega_1)$ are plotted for the 'stiff' elasto-acoustic element. As is shown in the previous section, the dispersion curves for the 'stiff' and the 'soft' elements have qualitatively the same pattern, so here the curves for the 'soft' element are not displayed. Curves 1–6 in Fig. 13a present a dependence of purely real wave numbers upon the frequency parameter. They specify propagating waves. As is seen, at least two waves of this type (more precisely, two pairs of waves, which have the same wave number value and propagate in opposite directions) exist in this shell at any frequency. Curves 7, 8 in Fig. 13a and in Fig. 13b present four complex-valued wave numbers. Finally, in Fig. 13b curves 1–6 and 9, 10 display a dependence of the purely imaginary roots on the frequency parameter. They describe waves, which decay in a fluid-filled shell. In Fig. 14 a zoomed picture from Fig. 13a is shown to illustrate generation of the third propagating wave in vicinity of the cut-on frequency $\Omega_1 \approx 0.78$. The location of dispersion curves for a fluid-filled cylindrical shell vibrating at the breathing mode has been presented in Ref. [20] and there is a good agreement between them and the results reported in the present paper.

Actually, these diagrams are reproduced here for consistency and for comparison with a fluid-loaded plate.

Similar to the case of a plate element loaded by the layer of fluid, there are an infinite number of 'fluid-originated' curves, which co-exist with a few 'structure-originated' ones. There are also several substantial differences between dispersion curves for a plate with fluid loading and a shell with fluid loading, which should be discussed in detail. Firstly, there are two modes, which

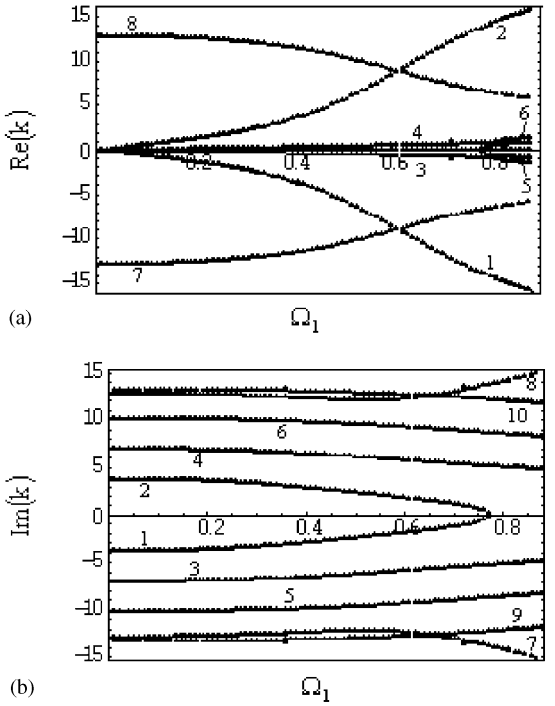

Fig. 13. Dispersion curves for a 'stiff' element of a periodic shell with heavy fluid loading: (a) purely real wave numbers and the real parts of the complex wave numbers; (b) purely imaginary wave numbers and the imaginary parts of the complex wave numbers.

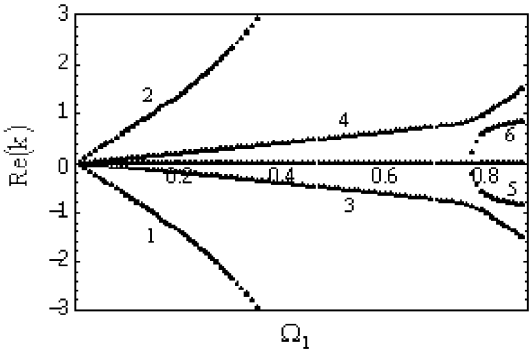

Fig. 14. Zooming of Fig. 13a.

propagate (naturally, both to the left and to the right) in a fluid-filled shell at any frequency, rather than a single mode in a plate with fluid loading. These free propagating waves have different structures. For a plate, it is the dominantly flexural 'structure-originated' free wave. For a shell, these are the dominantly longitudinal free wave and the dominantly acoustic free wave. As is shown in the analysis of wave propagation in an 'empty' shell, the dominantly longitudinal wave can propagate at any frequency. Propagation of this relatively long free wave is also supported in a fluid-loaded shell (see curves 3, 4 in Fig. 14). Besides this wave, the dominantly acoustic propagating wave also exists in this case, which is similar to the first duct mode in an absolutely rigid tube. In the low- frequency limit ($\Omega_1 \to 0$) the magnitudes of these wave numbers are scaled as $k = Z\Omega_1$, $Z = O(1)$. They may be asymptotically found from the reduced equation

$$-Z^2 + 1 + \nu^2 Z^2 + 2\beta \frac{R}{h} \frac{1 - Z^2}{1 - \bar{c}^2 Z^2} = 0. \tag{34}$$

It is easy to show that (i) both these waves have almost the same uniform profile of the distribution of a velocity potential in a fluid across the tube (there is a phase shift of $\pi/2$ between them) and (ii) nevertheless, they are orthogonal since the orthogonality condition for a fluid-filled shell involves all three components of each normal mode defined by Eq. (33). Secondly, unlike the previous case the two pairs of 'structure-originated' complex conjugate roots (which describe attenuated waves) exist in a shell with fluid loading over the whole considered frequency range. Finally, it appears that for the set of parameters chosen here, the third propagating wave cuts on at around $\Omega_1 \approx 0.78$ in this elasto-acoustic element. However, it is clear that if, for example, the graphs in Fig. 13b are extended further to the right, the same transformation should occur with the lowest branches of dispersion curves.

In all computations of wave propagation in a periodic shell with fluid loading, sixteen normal modes for each element are retained, i.e., $N_1 = N_2 = 2N_0 = 16$. In Fig. 15, characteristic curves are plotted for a shell composed by two sets of alternating elements with the parameters listed above. Curves 1 are reproduced from Fig. 3 and they present the dependence $\Omega_1(\mathrm{K}_B)$ for a shell without fluid loading. Curves 2 are plotted for a fluid-filled shell. Fluid parameters are the same as in Section 4, $\rho = 0.128$, $\bar{c} = 0.307$. They specified a steel shell filled by water. The band gaps zone in a fluid-loaded periodic cylindrical shell is shown in Fig. 15 and as is seen, the first band gap has practically disappeared due to the presence of a fluid, $0.861 < \Omega_1 < 0.864$, whereas the second band

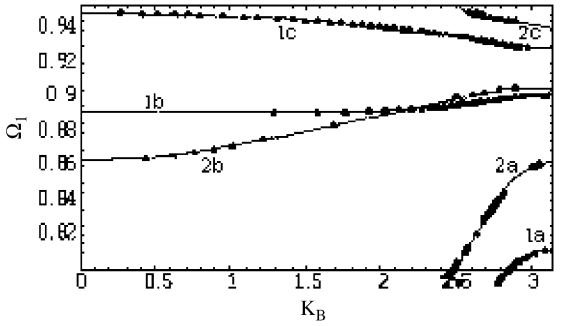

Fig. 15. Characteristic curves and band gaps in a periodic shell with fluid loading, $h_1/R = 0.01$, $\alpha = 1$, $\beta = 1$, $\lambda_1 = 2$, $\delta = 0.01$, $\chi = 0.01$, $\rho = 0.128$, $\bar{c} = 0.307$.

gap is slightly shifted upwards, $0.908<\Omega_1<0.942$ (compare with Table 1). Thus, at high frequencies, characteristic curves cover practically the whole frequency range and band gaps, in effect, disappear.

The reported results have a simple physical explanation. As is shown in Section 3, the first branch of characteristic curve describes propagation of a dominantly longitudinal wave in an empty cylindrical shell. Such a wave is characterized by small participation of the flexural component of a displacement field. When a shell is filled with water, propagation of this wave is also very slightly affected by the presence of a fluid and location of the relevant characteristic curve remains practically the same as in the case of an empty shell. The generation of band gaps due to the discontinuity in shell's parameters in a fluid-loaded shell is less pronounced than in a shell without fluid loading because the propagating dominantly acoustic wave co-exists with this longitudinal wave in each elasto-acoustic element at any frequency.

This also explains the principal difference between the results obtained for a plate loaded by a layer of fluid and for a fluid-filled cylindrical shell. In the former case, fluid loading has a very strong influence on location of characteristic curves because there is only one flexural wave, which propagates in a plate both with and without fluid loading at any frequency. The location and width of band gaps for a plate with fluid loading are very different from those without fluid loading due to the strong fluid–structure coupling in such a wave. In the case of a shell, the role of fluid is shown to be insignificant in a low-frequency region because the wave propagation is governed by the longitudinal deformation of a shell, which does not interact strongly with an acoustic medium and by the acoustical 'duct mode', which also does not strongly interact with a shell.

6. Conclusions

An investigation has been carried out into wave propagation phenomena in periodic elastic structures with and without heavy fluid loading. In the case of a periodic plate made up of two sets of alternating elements without fluid loading, an exact solution of the problem of the free wave propagation was obtained and the location of the first and the second band gaps was studied as a function of the stiffness ratio parameter. It was found that the second band gap vanishes at some critical magnitudes of the stiffness ratio. Another conclusion derived from this part of the paper is that for any given parameters of 'stiff' elements of a periodic plate and for any given frequency band it is always possible to choose the parameters of soft 'gaskets' to achieve the stop band effect. Furthermore, an exact solution was obtained for propagation of an axisymmetric wave in a periodic cylindrical shell without fluid loading. The structure of dispersion diagram was analyzed and the location of band gaps was studied as a function of the thickness parameter. Two elementary models are suggested to explain main phenomena of wave propagation in this case.

For the periodic plates and cylindrical shells with heavy fluid loading, an approximate solution was obtained in the form of expansion on normal modes of the coupled elasto-acoustic elements and the role of an acoustic medium was assessed. It was found that in general the presence of a fluid makes the band gaps narrower and, in certain situations, eliminates them completely. This result, which seems intuitively rather obvious, is quantified in several examples. In addition, the qualitative difference between wave guide properties of a fluid loaded periodic plate considered in

the framework of classic Kirchhoff theory and a fluid loaded periodic cylindrical shell considered in the same framework is explained.

References

[1] M. Cremer, M. Heckl, E.E. Ungar, *Structure-Borne Sound*, Springer, Berlin, 1987.
[2] Yu.I. Borbovnitski, M.D. Genkin, *Wave Propagation in Structures Composed by Thin-walled Rods and Plates*, Nauka, Moscow, 1974 (in Russian).
[3] D.J. Mead, Wave propagation in continuous periodic structures. Research contributions from Southampton, 1964–1995, *Journal of Sound and Vibration* 190 (1996) 495–524.
[4] E.E. Ungar, Steady state responses of one-dimensional periodic flexural systems, *Journal of the Acoustical Society of America* 39 (1966) 887–894.
[5] M.M. Siglas, E.N. Economou, Elastic and acoustic wave band structure, *Journal of Sound and Vibration* 158 (1992) 377–382.
[6] J. Wej, M. Petyt, A method of analyzing finite periodic structures, part 2: comparison with infinite periodic structure theory, *Journal of Sound and Vibration* 202 (1997) 571–583.
[7] J.-H. Lee, J. Kim, Sound transmission through periodically stiffened cylindrical shells, *Journal of Sound and Vibration* 251 (2002) 431–456.
[8] M.M. Siglas, E.N. Economou, Elastic waves in plates with periodically placed inclusions, *Journal of Applied Physics* 75 (1994) 2845–2850.
[9] C.G. Poulton, A.V. Movchan, R.C. McPhedran, N.A. Nicorovici, Y.A. Antipov, Eigenvalue problems for doubly periodic elastic structures and phononic band gaps, *Proceedings of Royal Society of London A* 456 (2000) 2543–2559.
[10] J.S. Jensen, Phononic band gaps and vibrations in one- and two-dimensional mass–spring structures, *Journal of Sound and Vibration* 266 (2003) 1053–1078.
[11] C. Kittel, *Introduction to Solid State Physics*, 7th Edition, Wiley, New York, 1996.
[12] D.G. Crighton, et al., *Modern Methods in Analytical Acoustics, Lecture Notes*, Springer, Berlin, 1992.
[13] L.S. Pontryagin, *Ordinary Differential Equations*, Nauka, Moscow, 1965 (in Russian).
[14] M.I. Rabinovich, D.I. Trubetskov, *Introduction to a Theory of Waves and Oscillations*, Nauka, Moscow, 1984 (in Russian).
[15] S. Wolfram, *Mathematica: A System for Doing Mathematics by Computer*, Addison-Wesley, Reading, MA, 1991.
[16] V.V. Novozhilov, *Thin Shell Theory*, Second Edition, Noordhoff, Leiden, 1968.
[17] S.P. Timoshenko, *Vibration Problems in Engineering*, Van Nostrand, New York, 1955.
[18] S.V. Sorokin, Analysis of vibrations and energy flows in sandwich plates bearing concentrated masses and spring-like inclusions in heavy fluid loading conditions, *Journal of Sound and Vibration* 253 (2002) 485–505.
[19] S.V. Sorokin, Analysis of wave propagation in sandwich plates with and without heavy fluid loading, *Journal of Sound and Vibration* 271 (2004) 1039–1062.
[20] C.R. Fuller, The input mobility of an infinite cylindrical elastic shell filled with fluid, *Journal of Sound and Vibration* 87 (1983) 409–427.